Article

UDC 535.215; 539.23; 535.3; 535.3; 538.9
https://doi.org/10.31489/2025PH2/19-26

Received: 26.02.2025
Accepted: 01.04.2025

T.E. Seisembekova[1]✉, A.K. Aimukhanov[1], A.K. Zeinidenov[1], A.M. Alexeev[2], D.R. Abeuov[1]

[1]*Karaganda Buketov University, Scientific Center for Nanotechnology and Functional Nanomaterials, Karaganda, Kazakhstan;*
[2]*eKazan Federal University, Kazan, Russia*

The effect of $MoSe_2$ nanoparticles on the properties ZnO electron transport layer of organic solar cell

This study investigates the impact of $MoSe_2$ nanoparticle doping on the structural, optical, and electrical properties of the ZnO electron transport layer (ETL), as well as its effect on the efficiency of organic solar cells (OSCs). ZnO:$MoSe_2$ composites were synthesized using the sol-gel method, and their morphology was analyzed by transmission electron microscopy (TEM) and scanning electron microscopy (SEM). Optical studies revealed an increase in the bandgap width and enhanced defect-related emission, indicating improved charge carrier dynamics. Electrical measurements confirmed increased conductivity and reduced charge recombination with the addition of $MoSe_2$. Organic solar cells based on ZnO:$MoSe_2$ demonstrated enhanced photovoltaic performance compared to pure ZnO devices. The optimal device was achieved at $MoSe_2$ concentration of 8 %, where the short-circuit current density (Jsc) increased from 7.25 mA/cm² to 10.02 mA/cm^2, the fill factor (FF) improved from 0.37 to 0.52, and the power conversion efficiency (PCE) rose from 0.7 % to 3.3 %. These results confirm the potential of ZnO:$MoSe_2$ nanocomposites for high-performance optoelectronic and photovoltaic devices.

Keywords: ZnO, $MoSe_2$, composite film, surface morphology, optical and impedance spectroscopy

✉*Corresponding author*: Seisembekova Togzhan, tosh_0809@mail.ru

Introduction

Enhancing the performance of photovoltaic devices can be achieved by incorporating 2D materials, which exhibit unique optical and electronic properties. Due to their ease of fabrication and processing, environmental friendliness, stability, and chemical compatibility with other materials in composites, 2D materials are widely used in photovoltaics as efficient transport layers. Among these 2D structures, transition metal dichalcogenides (TMDs) stand out due to their high charge carrier mobility (10–10^3 cm$^2\cdot$V$^{-1}\cdot$s^{-1}), transparency in the visible spectrum, and direct bandgap at the monolayer level. Integrating such structures into organic solar cells enables tuning of the bandgap, physical and chemical properties, and formation of van der Waals heterojunctions with other materials used in solar cells. These advantages make TMDs promising candidates for composite photovoltaic devices [1–5].

The 2D TMDs such as MoS_2, $MoSe_2$, and WSe_2 offer the possibility of tuning the bandgap and chemical properties and creating various van der Waals heterostructures with other materials. Due to their unique monolayer structure, the unshared electron pairs of S and Se atoms can facilitate fast charge transport, thereby increasing charge carrier mobility [6, 7].

However, using $MoSe_2$ nanoparticles alone does not form a continuous layered structure. Thus, we incorporated them into a ZnO layer synthesized via the sol-gel method to create a suitable composite electron transport layer for high-performance photovoltaic devices. The effect of ZnO doped with 2D TMD nanoparticles on the morphological, optical, and electrical transport properties remains insufficiently studied.

In this study, nanocomposite structures of ZnO doped with $MoSe_2$ were fabricated. The resulting ZnO:$MoSe_2$ thin films were used as electron transport layers (ETL) in organic solar cells (OSCs). The influence of $MoSe_2$ content, morphology, and nanocomposite ETL structure on charge transport and photovoltaic properties was thoroughly investigated. Few studies have been published on the fabrication of solar cells based on ZnO:$MoSe_2$ nanocomposite films. This work demonstrates that adding $MoSe_2$ nanoparticles to the ZnO-based ETL significantly improves solar cell efficiency.

Experimental

The ZnO precursor solution was prepared by dissolving 98.7 mg of zinc acetate (Zn(CH3COO)2, 99.9 % purity, Sigma-Aldrich) in 1 ml of isopropanol (99.9 % purity, Sigma-Aldrich). To enhance the solubility of zinc acetate in isopropanol, 75 μl of monoethanolamine was added to the solution. The final solution was stirred at 60 °C for 2 hours and then left at room temperature for 24 hours.

$MoSe_2$ nanoparticles were obtained by ablation using a solid-state Nd:YAG laser (SOLAR LQ 529, λ = 532 nm, E = 193 mJ, τ = 20 ns) in isopropanol. The concentration of $MoSe_2$ powder was 0.5 % of the total alcohol volume. Ablation times ranged from 10 to 30 minutes. To create ZnO:$MoSe_2$ nanocomposite films, nanoparticles were added to the ZnO solution in various concentrations from 2 % to 10 %. The nanoparticle concentration in the solution was calculated based on the density of the material according to the formula:

$$C_{NP} = \frac{C_{\mathrm{MoSe_2}}}{m_{NP} \cdot N_A} = \frac{C_{\mathrm{MoSe_2}}}{\rho_{\mathrm{MoSe_2}} \cdot V_{NP} \cdot N_A} = \frac{\frac{m_{\mathrm{MoSe_2}}}{V_{sol} M_{\mathrm{MoSe_2}}}}{\rho_{\mathrm{MoSe_2}} \cdot \frac{4\pi r^3}{3} \cdot N_A} \ (\mathrm{mol/l}), \quad (1)$$

where: C_{NP} — nanoparticle concentration; $C_{\mathrm{MoSe_2}}$ — concentration of the substance in solution before laser ablation of the substance $MoSe_2$; m_{NP} — average nanoparticle mass; N_A — Avogadro's number; $\rho_{\mathrm{MoSe_2}}$ — the density of matter is $MoSe_2$; V_{NP} — the volume of an average nanoparticle; $m_{\mathrm{MoSe_2}}$ — weight of the substance $MoSe_2$; V_{sol} — volume of solvent used in laser ablation; $M_{\mathrm{MoSe_2}}$ — molar mass of a substance $MoSe_2$; r — the radius of the average nanoparticle.

The ZnO:$MoSe_2$ nanocomposite films were deposited on substrates by spin coating at 4000 rpm. The films were annealed at 150 °C for 10 minutes to ensure complete solvent evaporation.

Results and discussion

Figure 1 shows the SEM images of pure ZnO and ZnO:$MoSe_2$ nanocomposite films deposited on a glass substrate. The nanocomposite structures exhibit a uniform distribution of nanoparticles across the ZnO surface, indicating high synthesis quality and sample homogeneity. The average nanoparticle size ranges from 30 nm to 80 nm.

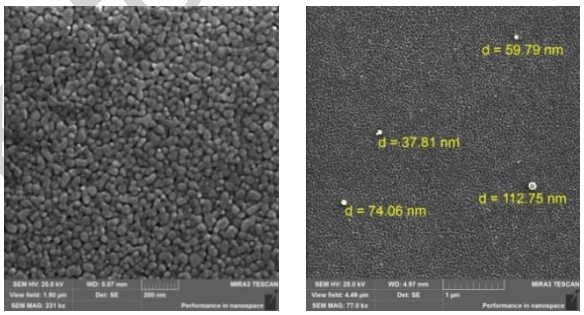

a) *b*)

Figure 1. SEM images of surface morphology (*a*) ZnO and (*b*) ZnO:$MoSe_2$ nanocomposite film

Morphological analysis revealed that the grain structure of pure ZnO differs significantly from that of the doped composites. In pure ZnO, the grains exhibit a well-defined crystalline structure, while in the doped samples, the ZnO grains become smaller. Smaller grains and increased grain boundary density enhance light scattering, increasing its path length and absorption probability, thereby improving photogeneration efficiency. Doping with $MoSe_2$ nanoparticles increases the number of nucleation sites, enhancing the distribution of active sites and improving electron and hole generation.

The quantitative content of $MoSe_2$ nanoparticles in ZnO was determined using EDX analysis (Fig. 2). The composite film contains elements such as Mo, Se, Zn, and O. As the nanoparticle concentration increases, the corresponding element concentrations also rise.

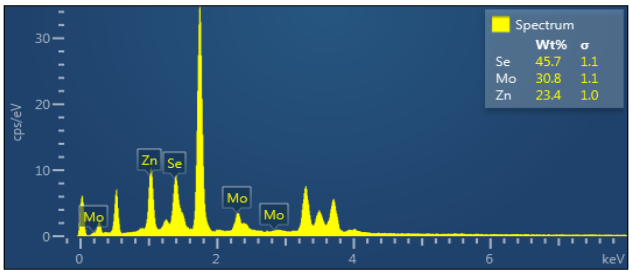

Figure 2. EDX analysis of nanoparticles $MoSe_2$

Figure 3 presents TEM images of ZnO:$MoSe_2$ nanocomposite films, revealing that the incorporation of $MoSe_2$ nanoparticles improves the ZnO film's morphology and topology. The nanoparticles are well-distributed and possess good monodispersity with sizes ranging from 3 to 6 nm.

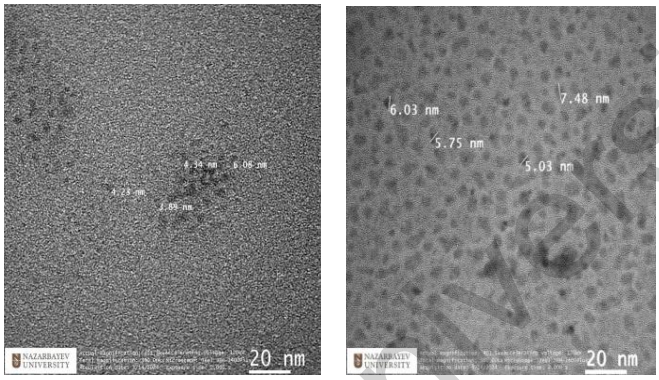

a) *b*)

Figure 3. TEM images of (*a*) pure ZnO and (*b*) ZnO:$MoSe_2$ nanocomposite films

The microstructure, morphology, and distribution of $MoSe_2$ nanoparticles in ZnO nanocomposite films have been analyzed by transmission electron microscopy (TEM). Figure 3 (*a* and *b*) shows TEM images of pure ZnO and nanocomposite ZnO films doped with $MoSe_2$ nanoparticles with a concentration of 8 %. Figure 3*a* shows an image of pure ZnO, which have a spherical shape, which is also confirmed by the results of the SEM analysis. Figure 3*b* shows that nanocomposite films of ZnO doped with $MoSe_2$ nanoparticles have a particle size in the range of 3-6 nm and have good monodispersity.

Figure 4 shows an AFM topographic image of ETL ZnO nanocomposite films doped with $MoSe_2$ nanoparticles. As can be seen from the figure, the $MoSe_2$ nanoparticles reduce the surface roughness.

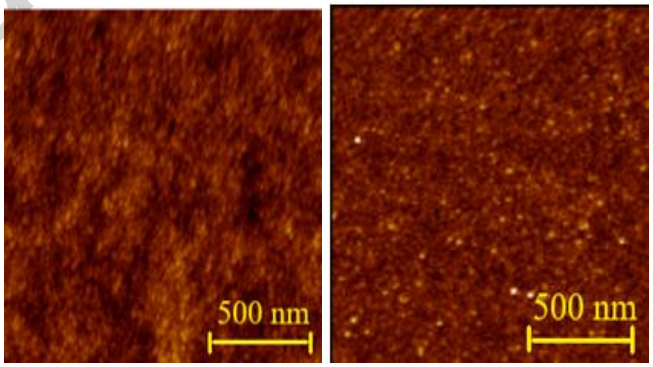

a) *b*)

Figure 4. AFM images of (*a*) pure ZnO and (*b*) ZnO:$MoSe_2$ nanocomposite films

AFM topographic images (Fig. 4) demonstrate that adding $MoSe_2$ nanoparticles reduces surface roughness (Ra). The Ra decreases from 2.8 nm to 0.8 nm with an 8 % $MoSe_2$ concentration, indicating

improved surface uniformity. However, at 10 % concentration, Ra significantly increases to 5.2 nm due to nanoparticle aggregation caused by Van der Waals forces [8].

Surface roughness reduction enhances molecular contact between the ZnO film and the active layer, improving interfacial dipole formation and reducing charge recombination.

The absorption spectra of ZnO and ZnO:$MoSe_2$ nanocomposite films are shown in Figure 5. As the nanoparticle concentration increases, the absorption intensity rises due to film thickness changes. Using Tauc plots, it was determined that the optical bandgap decreases from 3.24 eV to 3.07 eV as the $MoSe_2$ concentration increases up to 8 %, indicating improved crystallinity and reduced defect density.

At 10 % concentration, the bandgap widens to 3.26 eV due to increased structural defects and nonradiative recombination. These changes can be explained by an increase in the number of structural defects and nonradiative recombination that occur at high concentrations of nanoparticles. According to the study [9], such defects and recombination have a negative effect on the band gap. In addition, the possible formation of dichalcogenide clusters leads to phase separation and deterioration of the optical properties of the composite. Also, a high concentration of impurities can significantly change the ZnO crystal lattice, which further reduces the band gap [9].

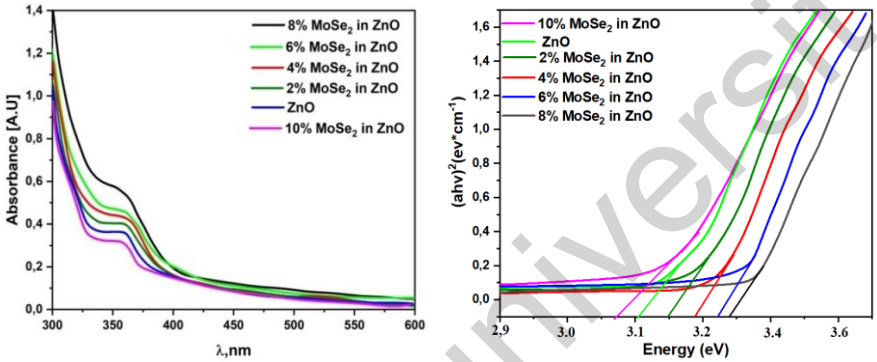

Figure 5. (*a*) Absorption spectra and (*b*) Tauc plots of ZnO:$MoSe_2$ nanocomposite films

The introduction of $MoSe_2$ nanoparticles can lead to an increase in the absorption coefficient of the composite, which causes enhanced absorption in the visible and near-infrared ranges [10]. It can also have an effect on the intensity and position of the ZnO luminescence bands.

The photoluminescence spectra of nanocomposite films were measured using an LQ529B laser as an excitation source with a wavelength of λ = 325 nm and an angle of incidence of 45° relative to the normal to the sample. The spectra were recorded using an Avantes AvaSpec-ULS2048CL-EVO spectrometer.

Figure 6 shows the change in the intensity of the photoluminescent (PL) peak at a concentration of 8 % of 2D TMDs nanoparticles obtained at room temperature (300 K).

It can be seen from the figure that the obtained samples show luminescence in the visible region. For all samples of nanocomposite films, a narrow band in the visible region of the spectrum in the range of 370–400 nm is observed in the photoluminescence spectra, which has a high luminescence intensity.

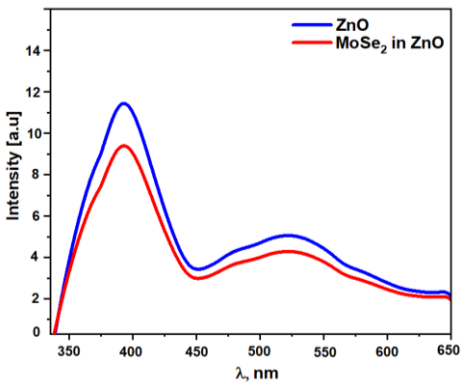

Figure 6. Photoluminescence (PL) spectra of nanocomposite films of ZnO doped with $MoSe_2$ nanoparticles

Visible radiation, known as green luminescence (PL) ZnO, was observed in all photoluminescence (PL) spectra, with a maximum at a wavelength of about 540 nm. The cause of EVIL is considered to be radiative transitions caused by deep energy levels of intrinsic defects, in particular oxygen vacancies.

Due to trap radiation or surface recombination, it appeared near 560 nm. Very few oxygen defects were present in the ZnO layers [11]. Therefore, we assumed that the effect of oxygen defects in the ZnO layers on the overall performance of the device would be negligible.

The photoluminescence intensity of a ZnO film containing a small number of dichalcogenide nanoparticles apparently decreased with increasing nanoparticle content, $MoSe_2$ nanoparticles with a concentration of 8 % are the lowest, which leads to better electron transfer to the FTO. Reducing the trap content in ETL solar cell devices would reduce the likelihood of interphase carrier recombination, and increase the Jsc and FF, thereby increasing the PCE of the device.

To study in detail the effect of $MoSe_2$ nanoparticles on the kinetics of electron transport and recombination in Oss, the OSCs impedance spectra were measured. The fitting and analysis of the spectrum parameters were carried out using the EIS-analyzer software package. Using this software, the values of the capacitance C and the values of R_1 and R_2 were calculated. The analysis of the impedance measurement results was carried out according to the diffusion-recombination model [12].

Further, Figure 7 shows the impedance spectra for nanocomposite ZnO films doped with $MoSe_2$ nanoparticles. According to the results of the study, the resistance of R_1 and R_2 for $MoSe_2$ nanoparticles also shows a significant decrease with an increase in the concentration of $MoSe_2$ nanoparticles to 8 %. As can be seen from Table 1, an increase in the concentration of $MoSe_2$ nanoparticles also leads to a decrease in recombination resistance.

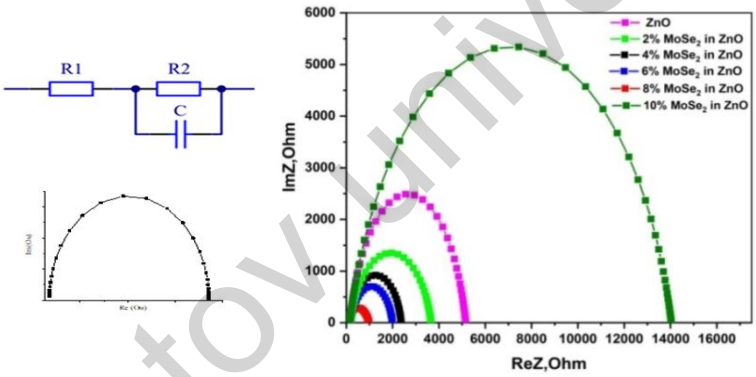

Figure 7. Effect of dichalcogenide nanoparticles on ZnO film impedance spectra

Table 1

The effect of $MoSe_2$ nanoparticles on the electrical transport characteristics of the ZnO film

Sample	R_1, Ohm	R_2, Ohm	C, 10^{-4} F	τ_D, c	Deff, ($cm^2 \cdot c^{-1}$)	μ, ($cm^2 \cdot V^{-1} \cdot c^{-1}$)
ZnO	131	5816	1.04	0.013	$2.2 \cdot 10^{-9}$	$0.8 \cdot 10^{-9}$
10 μl (2 %) $MoSe_2$ in ZnO	188	3446	2.3	0.043	$6.7 \cdot 10^{-10}$	$2.6 \cdot 10^{-8}$
20 μl (4 %) $MoSe_2$ in ZnO	143	2239	2.8	0.040	$7.2 \cdot 10^{-10}$	$2.8 \cdot 10^{-8}$
30 μl (6 %) $MoSe_2$ in ZnO	137	1810	3.3	0.045	$6.4 \cdot 10^{-10}$	$2.5 \cdot 10^{-8}$
40 μl (8 %) $MoSe_2$ in ZnO	89	954	5.4	0.048	$6.0 \cdot 10^{-10}$	$2.3 \cdot 10^{-8}$
50 μl (10 %) $MoSe_2$ in ZnO	146	13892	1.0	0.014	$1.9 \cdot 10^{-10}$	$0.7 \cdot 10^{-8}$

The analysis of the obtained data revealed a critical nanoparticle concentration (8 %) in the film at which the electrical transport properties of the ZnO:$MoSe_2$ composite film exhibit optimal performance. At this concentration, the film resistance and the charge transfer resistance at the ZnO/electrode interface decrease by 2 and 3.6 times, respectively, while the effective charge carrier mobility increases by 2.8 times.

It follows from the fitting data of the impedance spectra that **τ** has a maximum value for ZnO films. ZnO:$MoSe_2$ with a nanoparticle concentration of 8 %. The impedance analysis data is correlated with the VAC data. OSCs with ZnO:$MoSe_2$ 8 % of nanoparticles form ETL films with improved conductivity and less structural defects. A sharp deterioration in the photovoltaic parameters of OSCs with a ZnO concentration of

over 8 % of the $MoSe_2$ nanoparticle may be due to a violation of the integrity of the film, which causes holes and voids to form in the film, through which current leakage occurs.

In order to determine the effect of $MoSe_2$ nanoparticles on electronic transport, a polymer solar cell with an inverted structure was assembled in a polymer solar cell. Upon photoexcitation of the photoactive P3HT:IC60MA layer, an electron-holepair is formed, which then forms at the ZnO interface ZnO:$MoSe_2$/P3HT:IC60MA and P3HT:IC60MA/PEDOT:PSS decay into free charge carriers. Electrons are injected into the ETL layer of ZnO:$MoSe_2$ and the hole in the HTML layer is PEDOT:PSS.

Further, nanocomposite films of ZnO doped with $MoSe_2$ nanoparticles were used as electronic selective electrodes for organic solar cells based on the photoactive layer P3HT:IC60MA. The voltage curves of the obtained organic cells are shown in Figure 8.

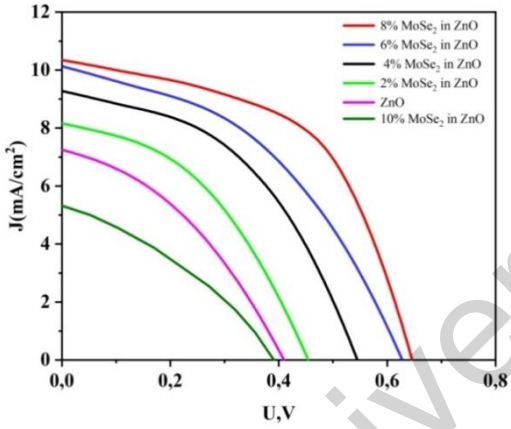

Figure 8. Volt-ampere characteristics of an organic solar cell of the structure FTO/ZnO:$MoSe_2$/P3HT:IC60MA/Ag

Table 2 shows the photovoltaic parameters of OSCs calculated on the basis of the VAC. As can be seen from Figure 8 and Table 2, the BAX parameters depend on the concentration of $MoSe_2$ nanoparticles. As the concentration of $MoSe_2$ increases to 8 %, the parameters of the VAC increase. A further increase in the $MoSe_2$ concentration leads to a decrease in the values of the VAC parameters. The data obtained correlate with the results of the morphology of the surface of composite films.

Table 2 shows the photovoltaic parameters of organic solar cells. All organic cells with $MoSe_2$ nanoparticles in the composition of ZnO showed improved values of Jsc and PCE compared to the ZnO based cell. Among them, the most optimal device was one in which the concentration of $MoSe_2$ nanoparticles was 8 %. Jsc increased from 7.25 mA/cm^2 to 10.02 mA/cm^2, FF increased from 0.37 to 10.52, and PCE increased from 0.7 to 3.3 %.

Table 2

Volt-ampere characteristics of organic solar cells

Sample	U_{oc} (V)	J_{sc} (mA/cm^2)	U_{max} (V)	J_{max} (mA/cm^2)	FF	PCE %
ZnO	0.27±0.01	7.25±0.05	0.27±0.01	4.07±0.05	0.37±0.01	0.7±0.05
10 µl (2 %) $MoSe_2$ in ZnO	0.45±0.01	8.19±0.05	0.31±0.01	4.76±0.05	0.40±0.01	1.4±0.05
20 µl (4 %) $MoSe_2$ in ZnO	0.54±0.01	9.29±0.05	0.38±0.01	5.78±0.05	0.43±0.01	2.1±0.05
30 µl (6 %) $MoSe_2$ in ZnO	0.62±0.01	10.1±0.05	0.42±0.01	5.78±0.05	0.42±0.01	2.6±0.05
40 µl (8 %) $MoSe_2$ in ZnO	0.64±0.01	10.2±0.05	0.49±0.01	7.02±0.05	0.52±0.01	3.3±0.05
50 µl (10 %) $MoSe_2$ in ZnO	0.21±0.01	5.31±0.05	0.21±0.01	3.25±0.05	0.33±0.01	0.3±0.05

The incorporation of $MoSe_2$ nanoparticles into ZnO significantly improves the morphological, optical, and electrical properties of the ETL in OSCs. The optimal performance was observed at an 8 % $MoSe_2$ concentration, where surface roughness was minimized, and conductivity was enhanced, resulting in a power conversion efficiency of 3.3 %. Further increasing the concentration to 10 % led to performance degradation due to nanoparticle aggregation and increased defects. These findings highlight the potential of ZnO:$MoSe_2$ nanocomposites for advanced photovoltaic applications.

Conclusions

The effect of $MoSe_2$ nanoparticles on the electron transport properties of the ZnO layer in polymer solar cells was studied. At the critical concentration of 8 % $MoSe_2$ nanoparticles in the ZnO:$MoSe_2$ nanocomposite films, the recombination rate at the ZnO:$MoSe_2$/photoactive layer interface decreases, while the transport of injected electrons improves. As a result, the power conversion efficiency (PCE) of the polymer solar cell with the FTO/ZnO:$MoSe_2$/P3HT:IC60MA/MoOx/Ag structure reached 3.3 %. The higher efficiency of the PSC with the ZnO:$MoSe_2$ electron transport layer containing diselenide nanoparticles compared to disulfide nanoparticles is attributed to the relative alignment of their conduction band positions.

Funding

This research is funded by the Science Committee of the Ministry of Science and Higher Education of the Republic of Kazakhstan (Grant No. AP19679109).

References

1 Cheng, R., Li, D., Zhou, H. et al. (2014). Electroluminescence and Photocurrent Generation from Atomically Sharp WSe_2/MoS_2 Heterojunction p–n Diodes. *Nano Lett., 14*(10), 5590–5597. DOI: 10.1021/nl502075n.

2 Lee, C.-H., Lee, G.-H., van der Zande, A.M. et al. (2014). Atomically thin p–n junctions with van der Waals heterointerfaces. *Nat. Nanotechnol., 9*(9), 676–681. doi: 10.1038/nnano.2014.150.

3 Deng, Y., Luo, Z., Conrad, N.J., et al. (2014). Black Phosphorus–Monolayer MoS2 van der Waals Heterojunction p–n Diode. *ACS Nano, 8*(8), 8292–8299. doi:10.1021/nn5027388.

4 Buscema, M., Groenendijk, D.J., Steele, G.A. et al. (2014). Photovoltaic effect in few-layer black phosphorus PN junctions defined by local electrostatic gating. *Nat. Commun., 5*(1), 4651-1-4651-28. doi: 10.1038/ncomms5651.

5 Lin, Y., Adilbekova, B., Firdaus, Y. et al. (2019). 17 % Efficient Organic Solar Cells Based on Liquid Exfoliated WS_2 as a Replacement for PEDOT:PSS. *Adv. Mater., 31*(46), 1902965-1-1902965-36. doi: 10.1002/adma.201902965.

6 Huang, Y.-J., Chen, H.-C., Lin, H.-K. et al. (2018). Doping ZnO electron transport layers with MoS_2 nanosheets enhances the efficiency of polymer solar cells. *ACS Applied Materials & Interfaces, 10*(23), 20196–20204. doi: 10.1021/acsami.8b06413

7 Chen, Y. Zeng, Herz, A., & Borchers, C. (2014). Inhibition of grain coarsening in nanocrystalline Fe-C alloys by interaction between carbon and grain boundaries. *Advanced Materials Research, 904*, 184–188. doi.org/10.4028/www.scientific.net/AMR.904.184

8 Jo, J., Pouliot, J.R., & Wynands, D. et al. (2013). Enhanced efficiency of single and tandem organic solar cells incorporating a diketopyrrolopyrrole-based low-bandgap polymer by utilizing combined ZnO/polyelectrolyte electron-transport layers. *Advanced Materials, 25*(34), 4783–4788. doi. 10.1002/adma.201301288

9 Cui, J. (2012). Zinc oxide nanowires. *Materialis Charact, 64*, 43–52. doi.org/10.1016/j.matchar.2011.11.017

10 Chiua, W.S., Khiew, P.S., & Clokea, M. et al. (2010). Photocatalytic study of two-dimensional ZnO nanopellets in the de-composition of methylene blue. *Chem. Eng. J., 158*, 345–352. doi:10.1016/j.cej.2010.01.052

11 Xie, Q., Dai, Z., & Liang, J. et al. (2005). Synthesis of ZnO three-dimensional architectures and their optical properties. *Solid State Commun, 136*, 304–307. doi:10.1016/j.ssc.2005.07.023

12 Omarbekova, G.I., & Aimukhanov, A.K. (2023). Effect of the thickness and surface interface of In_2O_3 films on the transport and recombination of charges in a polimer solar cell. *Bulletin of the University of Karaganda – Physics, 2*(110), 17–24. doi: 10.31489/2023PH2/17-24.

Т.Е. Сейсембекова, А.К. Аймуханов, А.К. Зейниденов, А.М. Алексеев, Д.Р. Абеуов

$MoSe_2$ нанобөлшектерінің органикалық күн элементтерінің ZnO электрон тасымалдаушы қабатының қасиеттеріне әсері

Мақалада $MoSe_2$ нанобөлшектерімен допирленген ZnO электрон-тасымалдаушы қабатының құрылымдық, оптикалық және электрлік қасиеттеріне, сондай-ақ органикалық күн элементтерінің тиімділігіне әсері зерттелді. ZnO:$MoSe_2$ композиттері золь-гель әдісімен синтезделіп, олардың морфологиясы ТЕМ және СЭМ микроскопиясы арқылы талданды. Оптикалық зерттеулер тыйым салынған аймақтың ені кеңейіп, ақаулық сәулеленудің күшейгенін көрсетті, бұл заряд тасымалдаушылардың динамикасының жақсарғанын білдіреді. Электрфизикалық өлшеулер $MoSe_2$ енгізу арқылы өткізгіштіктің артуы мен зарядтардың рекомбинациясының төмендеуін растады. ZnO:$MoSe_2$ негізіндегі органикалық күн элементтері таза ZnO негізіндегі құрылғылармен салыстырғанда жоғары фотоэлектрлік сипаттамалар көрсетті. $MoSe_2$ концентрациясы 8 % болған

құрылғы ең оңтайлы деп танылды, мұнда қысқа тұйықталу тогының тығыздығы (Jsc) 7,25 мА/см²-ден 10,02 мА/см²-ге дейін, толтыру коэффициенті (FF) 0,37-ден 0,52-ге дейін, ал энергияны түрлендіру тиімділігі (PCE) 0,7 %-дан 3,3 %-ға дейін артты. Алынған нәтижелер ZnO:$MoSe_2$ нанокомпозиттерінің жоғары тиімді оптоэлектрондық және фотогальваникалық құрылғыларда қолдануға тиімді екенін растайды.

Кілт сөздер: ZnO, $MoSe_2$, композиттік пленка, беттік морфология, оптикалық және импеданс спектроскопиясы

Т.Е. Сейсембекова, А.К. Аймуханов, А.К. Зейниденов, А.М. Алексеев, Д.Р. Абеуов

Влияние наночастиц $MoSe_2$ на свойства электронотранспортного слоя ZnO органического солнечного элемента

В статье исследовано влияние допирования наночастицами $MoSe_2$ на структурные, оптические и электрические свойства электронно-транспортного слоя ZnO, а также на эффективность органических солнечных элементов. Композиты ZnO:$MoSe_2$ были синтезированы методом золь-гель, их морфология проанализирована с использованием ТЕМ и СЭМ микроскопии. Оптические исследования показали увеличение ширины запрещённой зоны и усиление дефектной эмиссии, что свидетельствует об улучшенной динамике носителей заряда. Электрофизические измерения подтвердили увеличение проводимости и снижение рекомбинации зарядов при введении $MoSe_2$. Органические солнечные элементы на основе ZnO:$MoSe_2$ продемонстрировали повышенные фотоэлектрические характеристики по сравнению с устройствами на основе чистого ZnO. Наиболее оптимальным оказалось устройство с концентрацией $MoSe_2$ 8 %, где плотность тока короткого замыкания (Jsc) увеличилась с 7,25 мА/см² до 10,02 мА/см², коэффициент заполнения (FF) с 0,37 до 0,52, а эффективность преобразования энергии (PCE) с 0,7 % до 3,3 %. Полученные результаты подтверждают перспективность нанокомпозитов ZnO:$MoSe_2$ для применения в высокоэффективных оптоэлектронных и фотогальванических устройствах.

Ключевые слова: ZnO, $MoSe_2$, композитная пленка, морфология поверхности, оптическая и импедансная спектроскопия

Information about the authors

Seisembekova, Togzhan *(corresponding author)* — Master, Department of Physics and Nanotechnology, Karaganda Buketov University, Karaganda, Kazakhstan; e-mail: tosh_0809@mail.ru; ORCID ID https://orcid.org/0000-0002-1497-0759

Aimukhanov, Aitbek — Candidate of Physical and Mathematical Sciences, Associate professor, Professor of the Department of Radiophysics and Electronics, Leading Researcher, , Scientific Center for Nanotechnology and Functional Nanomaterials, Karaganda Buketov University, Karaganda, Kazakhstan; e-mail: a_k_aitbek@mail.ru; ORCID ID https://orcid.org/0000-0002-4384-5164. Scopus Author ID-35321945000

Zeinidenov, Assylbek — PhD, Associate professor, Dean of the Physical-Technical Faculty, Leading Researcher, Scientific Center for Nanotechnology and Functional Nanomaterials, Karaganda Buketov University, Karaganda, Kazakhstan; e-mail: asyl-zeinidenov@mail.ru; ORCID ID https://orcid.org/0000-0001-9780-5072. Scopus Author ID-56386144000

Alexeev, Alexandr — Candidate of Physical and Mathematical Sciences, eKazan Federal University, Kazan, Russia; e-mail: alalrus@mail.ru; Researcher ID — A-8526-2012; ORCID ID https://orcid.org/0000-0002-2800-6047

Abeuov, Dosmukhammed — Junior researcher, Scientific Center for Nanotechnology and Functional Nanomaterials, Karaganda Buketov University, Karaganda, Kazakhstan; e-mail: Dsk-02@mail.ru; ORCID ID https://orcid.org/0009-0003-1434-6328